

Electronic structure in quasicrystalline compounds and related crystals

This article has been downloaded from IOPscience. Please scroll down to see the full text article.

2002 J. Phys.: Condens. Matter 14 R789

(<http://iopscience.iop.org/0953-8984/14/31/201>)

View [the table of contents for this issue](#), or go to the [journal homepage](#) for more

Download details:

IP Address: 171.66.16.96

The article was downloaded on 18/05/2010 at 12:19

Please note that [terms and conditions apply](#).

TOPICAL REVIEW

Electronic structure in quasicrystalline compounds and related crystals

Esther Belin-Ferré

Laboratoire de Chimie-Physique, Matière et Rayonnement (UMR 7614 CNRS-UPMC),
11 Rue Pierre et Marie Curie, F-75231 Paris Cedex 05, France

E-mail: belin@ccr.jussieu.fr

Received 22 May 2002

Published 24 July 2002

Online at stacks.iop.org/JPhysCM/14/R789

Abstract

This article reviews and discusses the most relevant results achieved over recent years from the study of the electronic structure of quasicrystals (QCs) and related alloys using basically densities-of-states calculations and the x-ray emission, x-ray absorption, and photoemission spectroscopic techniques, in agreement with information obtained by other experimental means. It focuses on Al-based systems, the most widely analysed so far, and also reports data for Zr–Ni–Ti as well as Mg-based compounds. The present knowledge of QCs and approximants as compared to conventional crystals of the same phase diagrams may be summarized as follows: (i) the occurrence of a pseudogap at the Fermi level that is also present at the very surface is well established for icosahedral QCs whose formation derives from both Hume-Rothery and Al–transition metal hybridization effects; (ii) the pseudogap does not exist in the total densities of states of decagonal QCs but always exists in the Al sub-bands; (iii) states in QCs and close approximants are of more localized-like character in the vicinity of the pseudogap at the Fermi level than in conventional intermetallics, and at greater distances, above as well as below the Fermi level, they are extended-like in character, signalling a clear tendency to weak electron localization especially effective on either side of the pseudogap. As a result, there is a progressive loss of the metallic character, that can be tuned intentionally, when going from usual crystals to approximants and QCs.

(Some figures in this article are in colour only in the electronic version)

1. Introduction

Quasicrystals (QCs) were first detected 20 years ago, thanks to the characteristics of their electron diffraction pattern that consists of numerous well ordered intense spots displaying fivefold symmetry, which was at that time in contradiction to the rules of crystallography

(Schechtman *et al* 1984, Schechtman and Blech 1985). The first quasicrystalline specimens were metastable compounds prepared using the melt spinning technique. Before long, a QC in the Al–Cu–Li system was identified (Dubost *et al* 1986) that was prepared using conventional casting and solidification methods, hence being a stable compound. A number of other stable quasicrystalline phases were then discovered. Many belong to the icosahedral group (fivefold symmetry) (Tsai *et al*, 1987, 1988, 1989, Tsai 1997 and references therein) but are also found with classically forbidden eightfold (Wang *et al* 1987), tenfold, (Bendersky 1985, Chattopadhyay *et al* 1985) and twelvefold (Ishimasa *et al* 1985) symmetry axes. The lack of translational periodicity occurs in three dimensions for icosahedral quasicrystals (i-QCs) and in two dimensions for decagonal compounds (d-QCs) that are periodic stackings of quasiperiodic planes. Soon, these observed unexpected atomic arrangements raised the questions of possible genuine properties and electronic structure for this new class of solids.

In fact, it was found that the electronic conductivity at low temperature for i-QCs behaves oppositely to that for usual metallic alloys, as it increases with temperature and decreases with improving degree of lattice perfection (Berger 1994). Also, the heat conduction at room temperature is quite small, comparable to that of zirconia (Perrot and Dubois 1993). Another important issue came from specific heat measurements that were interpreted in terms of low densities of electronic states at the Fermi level (E_F) (Wang *et al* 1988, Wang and Garoche 1993). In addition, the stable QCs are formed from elements with small differences in electronegativity and atomic radius, and for electron per atom ratio (e/a) values around 1.86. Friedel and Denoyer (1987) and Friedel (1988) suggested that QC compounds are Hume-Rothery (HR) phases. Indeed, HR alloys are conventional stable crystals made of elements having similar electronegativities and atomic radii, with nominal compositions such as e/a takes specific values: 1.36, 1.48, 1.54, 1.86, 2.10, . . . They also show a depletion of the electronic densities of states (DOS) at E_F , the so-called HR pseudogap that was interpreted by Jones in terms of an energy stabilization mechanism resulting from the scattering of the conduction electrons by the planes of the Brillouin zone (Jones 1937, 1962). For QCs, a ‘pseudo-Brillouin zone’ (PBZ) can be constructed from the most intense peaks of the diffraction pattern. Because of the lack of translational periodicity, the reciprocal space is extremely dense and the PBZ displays numerous facets. Accordingly, gaps open in many directions of the reciprocal space and one may expect a pseudogap to form at E_F .

With the aim of improving our knowledge of the actual electronic structure and seeking for possible features attached to the lack of translational periodicity, many investigations have been undertaken to probe the DOS from theoretical as well as from experimental standpoints. From studies of the energy spectrum for one- and two-dimensional quasiperiodic lattices, further extended to three-dimensional quasilattices, the energy spectrum seems to be singular continuous in all dimensions. Hence, in quasiperiodic systems, the wavefunctions should be critical and the corresponding electronic states neither extended nor localized (Sire 1994 and references therein, Macia and Dominguez-Adame 2000). Mayou (2000a, 2000b) showed that due to the dense character of the reciprocal space, waves do not propagate easily in the quasiperiodic medium, so the diffusion of wavepackets is neither ballistic nor diffusive. For real QCs, because of the breakdown of translational periodicity, DOS calculations have to be carried out on model structures that mimic the local order of the QC. They are also often applied to related crystalline structures, the so-called approximants, that are found near to the QC area in the phase diagram and therefore show similar local order and close atomic compositions (Quiquandon *et al* 1999, Boudard 2000). Note that in several cases the atomic structures of approximant crystals that involve a large number of atoms in the unit cells have been derived from the Rietveld method, thus allowing exact DOS calculations (Mizutani *et al* 2001). Such DOS calculations were extended to a series of Al–TM conventional intermetallics (Trambly

de Laissardière *et al* 1995a, 1995b, Trambly de Laissardière and Mayou 1997). The authors stressed the importance of the Al–TM hybridization at E_F ; they claimed that it should play a role in the formation of the pseudogap. On the other hand, many experimental techniques have been involved so far in the investigation of QCs DOSs. For comparison purposes, the same studies were carried out on approximants as well as on conventional crystals. Various spectroscopies have been utilized, as these techniques provide a direct insight into the occupied and unoccupied bands and the electronic interactions. The underlying principles of the techniques whose results are reported here are summarized as follows.

The soft x-ray emission spectroscopy (XES) and x-ray absorption spectroscopy (XAS) techniques probe separately s, p, d occupied and unoccupied states, respectively, around each component of a solid, because x-ray transitions involve the inner level of the solid and obey dipole selection rules (Agarwal 1979, Bonnelle 1987). Transition probabilities are constant or vary slowly within the energy range of a band; therefore, XES and XAS data are proportional to the probed occupied or unoccupied DOS, respectively. The energy resolution is often limited by the energy width L associated with the inner hole involved in the x-ray transition. L varies from less than 0.1 to several eV depending on the element studied and the level. For the 2p level, it is about 0.4–0.5 eV for Al and 0.45–0.6 eV for transition metal (TM) elements of the first series or Cu, about 2 eV for Pd and Ru, and even larger for Re (Krause and Oliver 1979). Although no absolute DOS values are deduced from the measurements, it is possible to compare the same spectra for a given element in different compounds. The energy of a transition is the difference between the energies of the initial and final states. Hence spectral distributions are obtained, each on its own x-ray transition energy scale. Description of the occupied and unoccupied bands on the same energy scale requires further adjustment. For instance, E_F may be set on each x-ray transition energy scale on the basis of complementary measurements, so that a picture of the occupied and unoccupied bands is achieved using the binding energy scale where E_F is the origin (Traverse *et al* 1988, Belin and Traverse 1991). Note that XES and XAS data generally refer to the bulk material, although information can also be obtained from thin layers just below the surface of a material.

Another quite popular technique is x-ray photoemission spectroscopy (PES). Here, photoelectrons are emitted by a solid illuminated with an incoming x-ray (XPS) or UV (UPS) radiation. Measurement of the kinetic energies of the photoelectrons makes it possible to deduce their binding energies, owing to proper calibration of the spectrometer. This technique is mainly sensitive to the surface of the solid since it is dependent on the mean free path of the escaping photoelectrons (Kunz 1979, Hüfner 1995). Binding energies of the electrons of the occupied band are obtained together, modulated by photoionization cross-sections (σ). In contrast, inner levels are probed separately. Cross-sections depend on energy and noticeably favour d and f states. Accordingly, although some site selectivity may be achieved in systems made from elements not too close to each other in the Mendeleev table, no information can be gained for s and p states in samples containing both ‘sp’ and TM (rare-earth) elements. For Al-based materials, this might be unfavourable since one expects extended states (s and p) to be more sensitive than localized ones (d) to modifications in the long-range arrangement of the constituent atoms. The resolution of XPS is usually about 0.4–0.8 eV. In UPS, it may be as small as 3–5 meV, which makes it possible to investigate valence band edges in detail.

Other techniques such as Auger spectroscopy (AS), electron energy-loss spectroscopy (EELS), and angle-resolved photoemission (ARPES) that directly maps k -vector variation at given energies, and tunnelling spectroscopy are also valuable for investigating the electronic structure of QCs. They are still nowadays less employed than XES, XAS, and PES which are the most commonly used techniques; therefore we shall not go into the details of their basic principles.

The present article aims at a review and a discussion of the most relevant information achieved over recent years from the study of the occupied and normally unoccupied bands using basically DOS calculations and the XES, XAS, and PES techniques quoted above. It will mainly focus on Al-based systems which are, from the electronic structure point of view, the most widely analysed so far. However, data for Zr–Ni–Ti as well as Mg-based compounds will also be mentioned. The article is organized as follows: section 2 will report a summary of results on bulk icosahedral Al–Mn, Al–Cu(Pd)(Fe, Mn, . . .), Zr–Ni–Ti, Mg-based systems, and related crystalline alloys. Section 3 will give an account of data relating to d-QCs. Results concerning the electronic structure of quasicrystalline surfaces will be presented in section 4. The origin of the pseudogap will be discussed in section 5. Finally, conclusions will be given in section 6.

2. Icosahedral quasicrystals

As already mentioned, the calculated DOSs refer to model structures that mimic the local order in QCs. Most have been obtained by means of the linear muffin-tin orbital method in the atomic sphere approximation (LMTO-ASA). In such calculations, the sphere radii are chosen such that the total volume of the spheres equals that of the solid with slight overlap between neighbouring spheres, in order to minimize the excess number of electrons in each atomic sphere.

The data obtained from experimental techniques, especially XES and XAS, have always been compared to the same type of data measured for the pure elements used as standards. For Al-based alloys, any change in the shape of the partial DOS of the probed samples with respect to pure Al, a free-electron metal, will inform us of possible modifications of their metallic behaviour. For pure fcc Al, the Al 3s–d spectral curve exhibits a sharp, narrow peak at E_F due to the presence of some states with a d-like character (Léonard 1978, Papaconstantopoulos 1986) and many-body effects (Nozières and de Dominicis 1969). The Al 3p distribution curve shows an abrupt arctangent-like edge at E_F followed by a parabolic-like fall in intensity towards higher binding energies with a monotonically decreasing tail (figure 1). The Fermi level is exactly at the inflexion point of the Al 3p edge (Rooke 1968, 1974). The Al p absorption curve displays an arctangent-like edge with the inflexion point set also at E_F .

For a meaningful comparison of the Al spectral curves of fcc Al and the various specimens, these are normalized to their maximum intensity. In such a procedure, for fcc Al, the intensity of the inflexion point at E_F is equal to half the maximum intensity of the 3p sub-band. On the binding energy scale this inflexion point is set at the origin. For the alloys, whatever they are, since there is no reason *a priori* for the crystalline or quasicrystalline alloys to be free-electron-like, we have determined the position of the Fermi edge independently from complementary measurements, as indicated above (Traverse *et al* 1988, Belin and Traverse 1991). Therefore, one expects the intensity at E_F , called I_{E_F} , to differ from and in fact be lower than the half-maximum intensity of the 3p sub-band, and to be moved by an amount δ away from the energy position of E_F . This notation is illustrated in figure 1.

(a) The Al–Mn(–Si) system

In 1982, Shechtman was investigating the solubility of manganese in aluminium using the melt-spinning technique when he observed the strange electron diffraction pattern displayed by the 75–25% Al–Mn phase which opened the era of QCs. The DOSs of the metastable i-Al–Mn and the i-Al–Mn–Si quasicrystalline compounds were the first ones calculated by Fujiwara (1989) and Fujiwara and Yokokawa (1991) (figure 2). The total and partial DOSs showed that

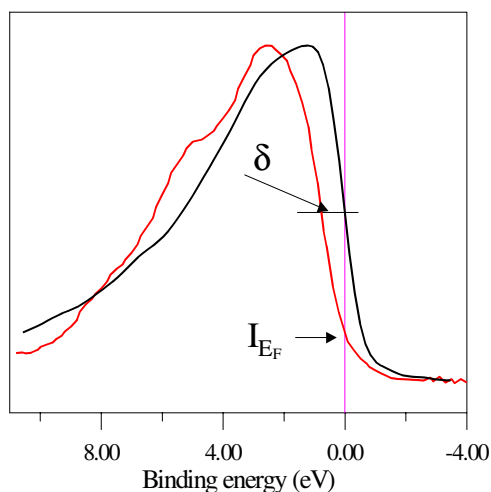


Figure 1. Parameters attached to the Al 3p distribution curve for Al-based phases: the thick dark curve is for fcc Al and the other one relates to an Al-based compound.

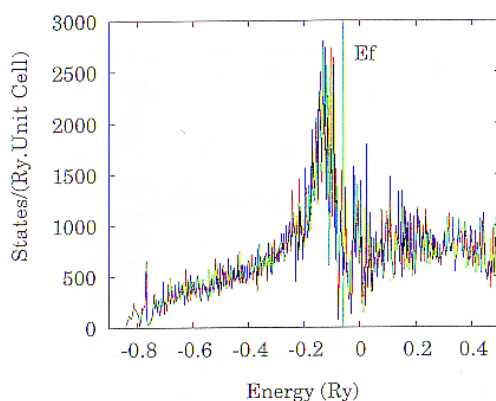


Figure 2. The total density of states in a model approximant of i-Al-Mn (Fujiwara *et al* 1993). The origin is set at the Fermi level.

Mn d states are dominant and set close to E_F , whereas the bottom of the total valence band, far away from E_F , retains a parabolic-like shape. These calculations, which did not involve Al 3d states as valence states, also displayed numerous narrow spikes about 10–20 meV wide and set E_F in a region of depleted DOS, namely close to a pseudogap. The authors assumed that both the spikes and the pseudogap at E_F should be general features of QCs. In addition, flat energy bands were found, especially around E_F , which led Fujiwara and co-workers to propose that the i-Al-Mn(-Si) compounds, although containing a high proportion of Al, would display a non-metallic behaviour.

Recently, the DOS of the ideal three-dimensional Penrose tiling was calculated with a resolution of 10 meV. The result showed no dense narrow spikes, whereas these are still present in the calculations of both a small approximant of the three-dimensional Penrose tiling and the ideal two-dimensional Penrose tiling (Zijlstra and Janssen 2000). The qualitative difference between these results and the previous ones is partly assigned by Zijlstra and Janssen to the small number of k -points that were involved in the calculation for the periodic approximants of

QCs by Fujiwara and co-workers. It is also to be noted that to date no experimental evidence of spikes in the DOS has been obtained whatever technique was used (Stadnik *et al* 1997, Schaub *et al* 1999). Therefore, nowadays, the spiky structure is questioned and no longer considered as being a signature of the quasiperiodic order.

Figure 3 shows a picture of the occupied Al and Mn sub-bands in Al_6Mn as obtained from XES measurements, adjusted on the binding energy scale, together with the total calculated DOS that is dominated by Mn d states. The same general distribution of the partial DOS is found for i-AlMn(Si) QCs (Bruhwiler *et al* 1988, Ederer *et al* 1988, Traverse *et al* 1988, Belin and Traverse 1991, Belin *et al* 1992, Dankhazi *et al* 1993). The experimental partial DOS curves show overlap between Mn d and Al s-d and p states in the vicinity of E_F that indicates states hybridization in this energy range. The shapes of the partial Al 3p and 3s-d states are reminiscent of those for fcc Al, but there is a slight depletion around E_F ; thus I_{E_F} in the Al 3p distribution is slightly reduced with respect to that for fcc Al: a small pseudogap forms at E_F . This is exemplified in figure 4 which shows the Al 3p distributions in i-Al-Mn and i-Al-Mn-Si as compared to that of fcc Al. I_{E_F} is found to be slightly lower and the distance δ is a little larger for the QCs than for crystalline Al_6Mn . For both i-Al-Mn and i-Al-Mn-Si, the Al 3s-d distribution curves display a peak just below E_F that is broader than that for pure fcc Al. Therefore, observation of the Al 3p and 3s-d sub-band shapes gives an indication that i-Al-Mn(-Si) compounds do not depart too dramatically from the metallic-like behaviour, in fair agreement with the DOS calculations quoted above. In fact, the resistivities of these QCs are around $100\text{--}200 \mu\Omega \text{ cm}$ at room temperature, i.e. similar to those of metallic glasses in the same systems (Berger *et al* 1993, Berger 1994). This is confirmed by the investigation of the unoccupied Al p band. The Al p spectral curves show a slight depletion just above the edge, which agrees with some loss of the free-electron behaviour in these systems (Bahadur *et al* 1987, Traverse *et al* 1988).

The spectral distribution of the Mn d states, located at about 1 eV below E_F for i-Al-Mn as well as i-Al-Mn-Si and the crystalline alloy, is narrower by about 0.6 eV with respect to that for pure Mn, observed in the same experimental conditions. We will come back later to this point.

(b) Al-Cu(Pd)-Li(transition metal) systems

The discovery of stable QCs by Dubost *et al* (1986) and Tsai *et al* (1987) gave a further impulse to the investigation of the electronic structure of i-compounds and related conventional crystals. Total and partial DOS calculations, generally using the LMTO-ASA or tight-binding LMTO methods, were carried out on many Al-Cu(Pd)-TM systems as well as on Zn-Mg-Y and Zr-Ti-Ni compounds. For Al-based alloys the new calculations accounted for Al 3s, 3p as well as 3d states as valence states together with d-s states for the TM, Cu, or Pd (Fujiwara *et al* 1989, 1993, Hafner and Krajci 1993, Trambly de Laissardière and Fujiwara 1994a, 1994b, Windisch *et al* 1994, Krajci *et al* 1995, Roche and Fujiwara 1998a, 1998b).

These calculations set occupied d TM states about 1 eV below E_F whereas 3d Cu (4d Pd) states, that are the dominant states in the DOS, lie in the middle of the band at about 4 eV below E_F . They confirmed the existence of a clear pseudogap at or very close to E_F as shown in figures 5 and 6, respectively, for the two approximants i-Al-Cu-Li (Fujiwara and Yokokawa 1991) and i-Al-Cu-Fe (Trambly de Laissardière and Fujiwara 1994a). The unoccupied band was found to be less intense than the occupied one, thus giving an asymmetric shape to the total DOS, in agreement with the structural model based on a clusters hierarchy proposed by Janot and de Boissieu (1994) for i-Al-Pd-Mn. The calculations also assessed the flatness of the dispersion relation curves near E_F . Finally, all calculated features are in line with the poor metallic character of the corresponding alloys (Berger 1994 and references therein).

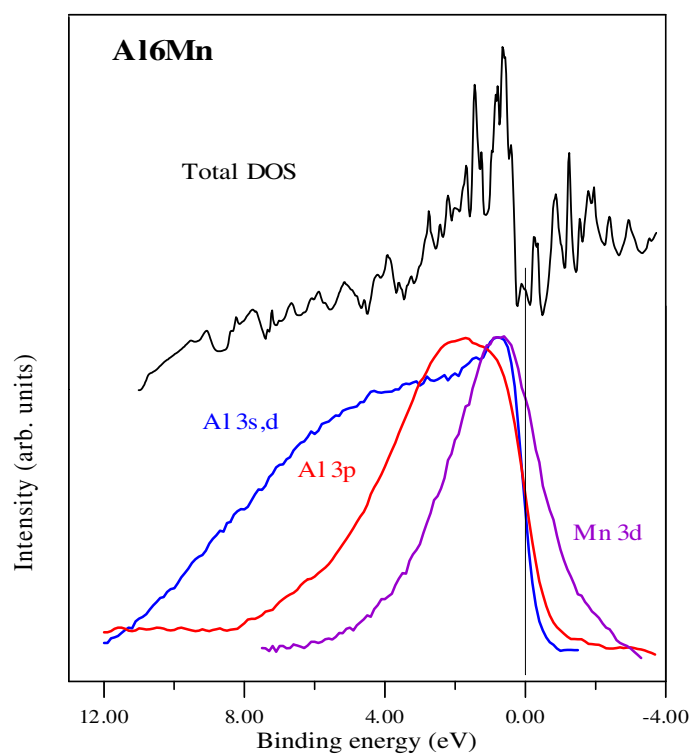


Figure 3. Calculated total DOS (upper curve) and experimental spectral curves for Al₆Mn (lower curves).

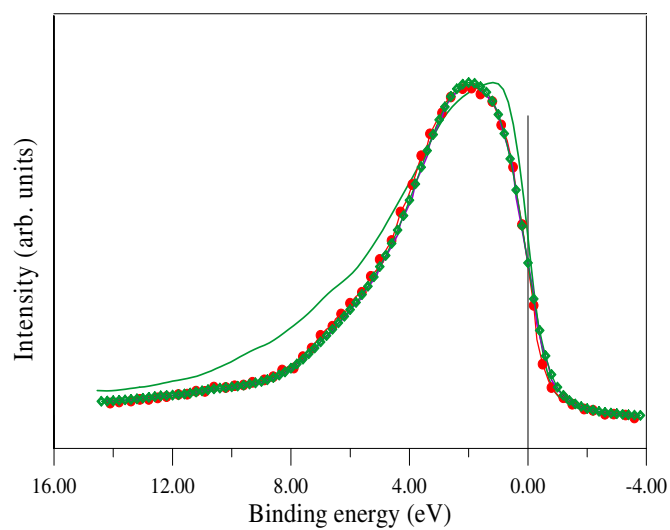


Figure 4. Al 3p distribution curves for fcc Al (full thin curve), i-Al-Mn (thick curve), and i-Al-Mn-Si (dotted curve).

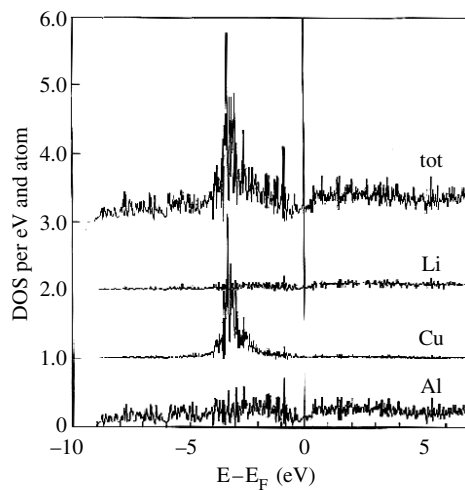


Figure 5. The LMTO calculation of the DOS of the R-approximant of i-Al-Cu-Li with 160 atoms in the unit cell (Windisch *et al* 1994).

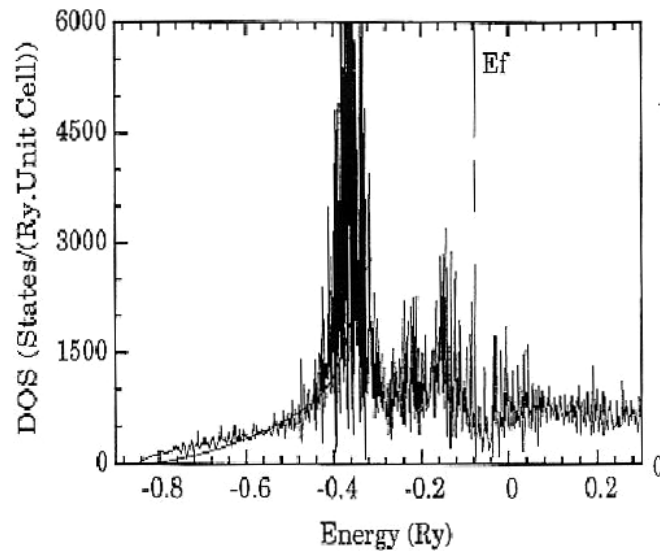


Figure 6. The total DOS in a model approximant of i-Al-Cu-Fe. The onset of intense peaks corresponds to Cu d states; Fe d states are close to the Fermi level. Note that here E_F (vertical upper line) is not set at the origin (Trambly de Laissardière and Fujiwara 1994a).

Krajci *et al* (1995) investigated in detail the formation of the minimum in the DOS at E_F as a function of increasing order of the model Al-Pd-Mn approximants—i.e. going closer and closer to the actual QC. They found that the pseudogap was neither very marked nor exactly at E_F for the low-order approximants, but was more pronounced and moved progressively towards E_F with increasing order (figure 7). Note that the pseudogap at E_F was also found in DOS calculations for usual intermetallics belonging to the same phase diagrams as the i-phases (Trambly de Laissardière *et al* 1995a, 1995b, Belin-Ferré *et al* 1997, Fournée *et al* 1999). This will be addressed in section 4.

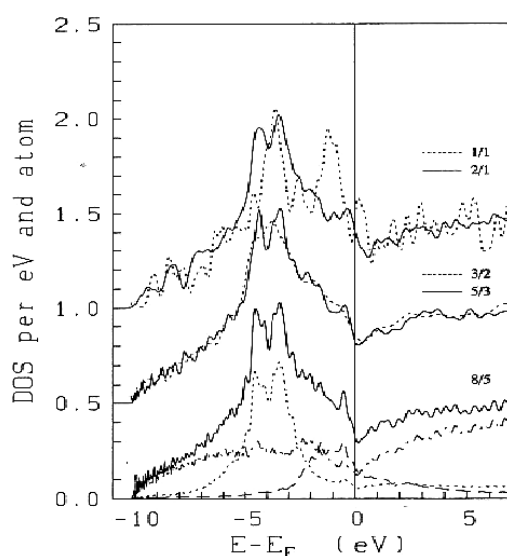


Figure 7. Total LMTO-TB DOSs for a series of approximants of i-Al-Pd-Mn. The partial Al, Pd, and Mn DOSs are shown as dashed, dotted, and dash-dotted curves respectively (Krajci *et al* 1995). The 8/5 approximant is the closest to the i-compound.

Analysis of inner level distributions from PES experiments revealed shifts towards high binding energies ranging from 0.2 to 0.6 eV for the Al $2p_{3/2}$ level when going from pure fcc Al to crystalline intermetallics and QCs, which confirms that electronic interactions are stronger in QCs than the crystalline counterparts (Terauchi *et al* 1996a, 1996b, Belin *et al* 1992, 1994, Belin-Ferré *et al* 1996). For Cu $2p_{3/2}$ and Pd $3d_{5/2}$ levels, shifts as large as 1–2 eV are observed with reference to the pure metals. Therefore one can infer that Cu and Pd interact strongly with Al. Interaction with TM (Fe, Ni, Co, Ru, Re, ...) inner levels does not affect them as much since the inner levels are not critically shifted in the alloys with respect to the pure metals. This latter result is consistent with data from XES and PES measurements for QCs, approximants, and conventional crystals of close nominal composition, which have shown that the TM d states are present in the range 1–2 eV below E_F and hence not very far away from their positions in the elements (Stadnik *et al* 1997 and references therein, Belin-Ferré 1999 and references therein).

Strong deviation with respect to free-electron elements was found from high-resolution valence band edge PES investigations for real QCs (Mori *et al* 1991, Stadnik *et al* 1997, Neuhold *et al* 1998) as shown in figure 8. This figure compares the valence band edges in i-AlCuFe, fcc Al, and pure Au (Mori *et al* 1991). The slope of the edge for i-Al-Cu-Fe departs strongly from those for the two other metals; accordingly, this QC does not behave as a free-electron compound. In fact, i-Al-Cu-Fe, like other Al-Cu(Pd)-TM compounds, displays a very high resistivity both at room temperature and at low temperatures (Berger 1994).

XES measurements have indicated that the interaction between the relatively localized Cu(Pd) d states and the extended Al band results in an asymmetric distortion of the Al p and s-d sub-bands which split into bonding and anti-bonding parts located on both sides of the d distribution with a marked dip in the energy range of the maximum of the Cu(Pd) d state curve. The TM metal d states overlap with Al states near E_F . Accordingly the Al states within a few electron volts below E_F are essentially hybridized with d states—that is, of somewhat localized character. They are pushed away from E_F with respect to pure fcc Al, showing thus

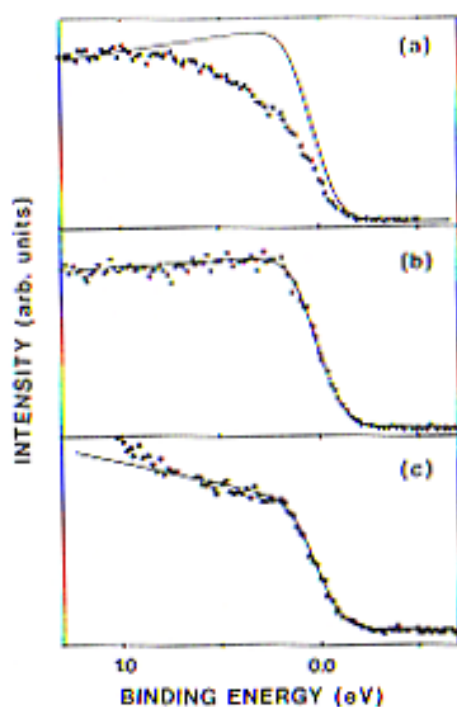


Figure 8. The PES valence band edge taken at an excitation energy of 40 eV for i-Al–Cu–Fe (a), fcc Al (b), and pure gold (c). The solid curves represent the edge calculated assuming that the sample behaves as a free-electron metal. Note the good fit between calculation and experiment for Al and Au.

a decrease in the intensity at E_F and a marked bending of the Al occupied band edges. Then a pseudogap at E_F is clearly present in the Al occupied states of these alloys. An example is given in figure 9 that shows the occupied band for i-Al–Cu–Fe reconstructed from XES partial electronic distributions adjusted to their maximum intensity on the binding energy scale. Note that the same general arrangement of the partial sub-bands holds for the Al–Cu–(Pd)–TM systems whatever their atomic structure. Differences are seen from one compound to another in the details of the various partial contributions. For instance, the shape of the Al 3p state distribution curve depends on the strength of the interaction between these states and the Cu or Pd d states. According to Terakura (1977) one expects the dip in the spectral curve to become more marked as the corresponding interacting states become more extended-like, on the one hand, and localized, on the other hand. Examination of the Al 3p spectral curves in various samples has led to the conclusion that the Al states tend to become progressively more and more localized when going from conventional crystals to approximants and QCs (Belin-Ferré *et al* 2000). Figure 10 which compares the Al 3p state distribution in i-Al–Cu–Fe, a rhombohedral approximant, and the Φ -Al₁₀Cu₁₀Fe phase illustrates the point: the dip around 4 eV below E_F is strongly marked for the conventional crystal, becomes a slightly contrasting shoulder for the approximant, and is even (slightly) less for the QC.

Comparison with calculated DOSs (see for instance Trambly de Laissardière and Fujiwara (1994a, 1994b), Trambly de Laissardière *et al* (1995b)) establishes that the Al 3s–d states in the energy range within 3 eV below E_F are significantly d-like, thus confirming the localized-like character in this energy range. Finally, the only Al extended states, whatever the specimen, are

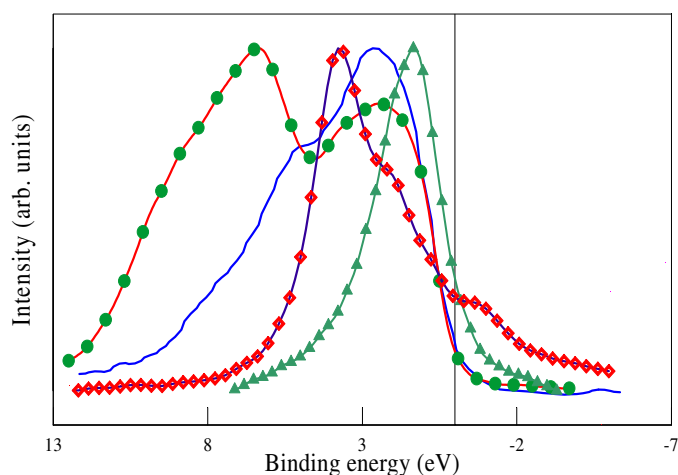


Figure 9. The valence band of *i*-AlCuFe. Al 3p states: full curve. Al 3s–d states: full dots. Cu 3d–4s states: diamonds. Fe 3d–4s states: triangles. For Cu and Fe, the transition probabilities mean that it is essentially d states that are probed by the experiments.

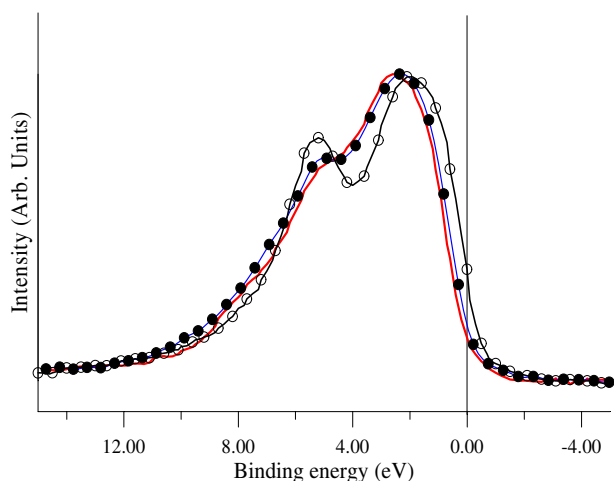


Figure 10. Al 3p states distribution curves for Φ -Al₁₀Cu₁₀Fe (open dots), the rhombohedral Al–Cu–Fe approximant (full dots), and the *i*-Al–Cu–Fe compound (full curve).

those of high binding energy that are pure *s* in character (Belin *et al* 1994, 1995, Belin-Ferré *et al* 1996).

Both the decrease of intensity and edge bending are more marked in the QCs than in their approximants and the conventional alloys. Figure 10 illustrates this point again: the intensity at E_F of the Al 3p state distribution curves, I_{E_F} , decreases from Φ -Al₁₀Cu₁₀Fe to the rhombohedral approximant and *i*-Al–Cu–Fe, while the maximum of the distribution progressively shifts from E_F . In addition, the pseudogap in the Al 3p distribution becomes more marked as the resistivity of the sample increases. For instance, the Al 3p I_{E_F} has been found to be about two times lower for highly resistive *i*-Al–Pd–Re (Belin *et al* 1995) than in *i*-Al–Cu–Fe (Belin *et al* 1992). For this latter compound it is about 30% of that

for fcc Al. Note that the resistivities at low temperature range from 5000 $\mu\Omega$ cm to about 1 Ω cm (not far from the metal–insulator transition) according to the degree of perfection of the quasicrystalline network, for i-Al–Cu–Fe and i-Al–Pd–Re respectively (Berger 1994, Préjean *et al* 2002, Delahaye and Berger 2002).

The overall shapes of the TM and Cu(Pd) occupied d distributions as probed by XES are similar for QCs and related crystals. As already mentioned above in section 2(a), the d bands are narrower by about 0.5–1 eV in the compounds with respect to the metal, consistently with the lack of same-type neighbour atoms in alloys and compounds as compared to the pure metals. This narrowing will be discussed in more detail in section 4. For i-Al–Cu–Fe, the Fe 3d state intensity at E_F was found to be lower than in pure Fe, in line with the presence of a pseudogap in the total DOS (Belin and Mayou 1993).

Above E_F , XAS experiments have indicated that unoccupied TM states of d–s character overlap with Al p states, whereas Cu(Pd) d–s states are found at a further distance, beyond about 2 eV, in agreement with partial DOS calculations. At larger energies all unoccupied states are mixed. The shapes of the TM and Cu(Pd) curves for the compounds are much less sharp and are broader than those for the pure metals (Sadoc *et al* 1993, Belin-Ferré *et al* 1996), which is ascribed to some filling of the d band as a result of hybridization with Al states. An important issue is that there is always some d character at E_F , since the conduction band is p, d–s hybridized near the edges and then becomes more s–p above about 5 eV from E_F .

The edges of the Al p spectral curves of the alloys are less abrupt than in fcc Al; in addition, they show a depletion in the energy range where the TM and Cu(pd) d states are present, namely around 2 eV above the edge, in line with sp–d interaction. These curves have been adjusted at E_F to the same intensity as the occupied Al 3p counterparts, assuming that the distribution of p character is a continuous function of the energy. The Al 3p sub-bands have all been normalized in the same way at their maximum intensity. Within this adjustment scheme, the occupied Al 3p and unoccupied Al p sub-bands cross each other at E_F . This gives a clear picture of the depletion of the Al p state distribution around E_F with respect to that of pure fcc Al and emphasizes the presence of a marked pseudogap and a strong asymmetry of the occupied and unoccupied Al p bands as seen in figure 11. In this figure, for clarity, only the Al 3p occupied sub-bands for pure fcc Al and the Al₂Ru compound studied for comparison purposes are shown (Belin-Ferré and Dubois 1996). This latter compound, according to DOS calculations by Nguyen Manh *et al* (1992), should display a real gap; some broadening due to instrumental constraints mean that in experiments it is seen as a wide low pseudogap Fournée *et al* (1997). Such a marked depletion of Al p states just above E_F has also been deduced from EELS measurements on quasicrystalline i-Al₆₅Cu₂₀Ru₁₅ samples (Terauchi *et al* 1996a, 1996b). It is worth noting that the flatter the Al p conduction band, the higher the resistivity of the sample at room temperature. Altogether, within the framework of the intensity adjustment mentioned above, one can follow in the plot of Al distribution curves of the occupied and unoccupied p states the variation of the free-electron-like character from sample to sample.

Finally, altogether there is experimental evidence that in the Al–Cu(Pd)–TM icosahedral phases both occupied and unoccupied states in the vicinity of E_F are d–p-like—i.e. rather localized-like in character—which is in agreement with the calculations of the energy spectrum quoted above. In contrast, states far from E_F —that is, far from the pseudogap energy range—are more extended-like, and even pure s at the bottom of the occupied band.

(c) Zr–Ti–Ni systems

The Ti–Zr–Ni system is interesting, as stable i-compounds as well as approximant phases exist. Furthermore, these materials store H reversibly, which makes them potentially promising for industrial use. Indeed, the as-cast stable Ti₄₅Zr₃₈Ni₁₇ approximant Laves phase as well as

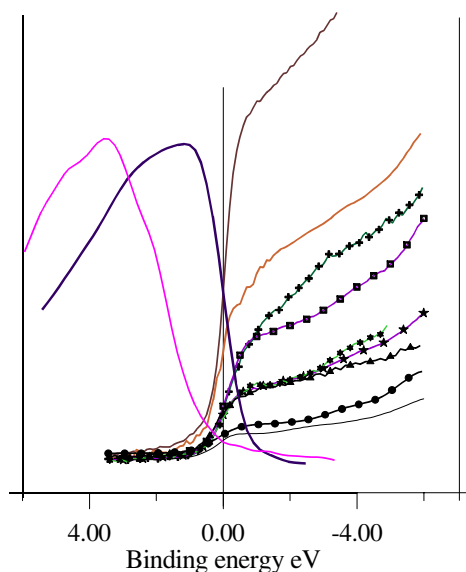


Figure 11. Left side of the figure: towards increasing energies, Al 3p curves for Al_2Ru and fcc Al. Right side, from top to bottom: Al p curves for fcc Al, $\omega\text{-Al}_7\text{Cu}_2\text{Fe}$, $\text{Al}_{13}\text{Fe}_4$, Al-Cu-Fe rhombohedral approximant, i-Al-Cu-Ru, i-Al-Cu-Fe, i-Al-Pd-Mn, i-Al-Pd-Re, and Al_2Ru . For the procedure of normalization of the intensity scale (vertical axis), see the text.

the stable annealed icosahedral $\text{Ti}_{45}\text{Zr}_{38}\text{Ni}_{17}$ compound accept H up to a H/metal ratio of 1.7 (Libbert *et al* 1993). Therefore, in addition to the usual investigation of the electronic structure, interest has been raised as regards H bonding in such solids.

A theoretical study of the electronic structure has been carried on through band-structure calculations for the 1/1 approximant $\text{W-Ti}_{52}\text{Zr}_{32}\text{Ni}_{16}$. These calculations used a density functional code with a plane-wave basis and ultrasoft pseudopotentials that for Ti and Zr involved the usual outer-shell states and also the 3p and 4p states, respectively, as valence states. For the pure elements the occupied band consists mainly of d states over about 4 eV below E_F , whereas s states of quite low intensity are present at about 3 and 4 eV from E_F for Ti as well as Zr and Ni, respectively (Belin-Ferré *et al* 2002). In binary TM alloys, hybridization effects in the occupied band induce a transition from a common-band regime, for small differences in energies of the atomic d states of the constituents, to a split-band regime when the energy distance in the d levels goes on increasing (Hausleitner and Hafner 1992). This effect is observed here since, in the W-phase, the total DOS is dominated by a wide complex d band. The partial occupied d DOSs of Ti and Zr have similar shapes and show complete mixing (hybridization); they spread over about 1 eV from E_F whereas the intense occupied Ni d sub-band is mostly located in an energy range from 2 to 3 eV from E_F (figure 12). The empty states are basically d in character over $E_F + 2$ eV with some contribution of p states. This calculation indicates a strong interaction between Ni atoms on the one hand and Zr and Ti atoms on the other hand. Since Ni has a higher electronegativity than the other two atoms, a large charge transfer occurs from the Ti and Zr atoms towards Ni atoms (Belin-Ferré *et al* 2002).

Measurement of the binding energies of Ti, Zr, and Ni $2p_{3/2}$ core levels in i- $\text{Ti}_{53}\text{Zr}_{27}\text{Ni}_{20}$ in PES experiments confirmed the sensitivity of Ni DOSs to alloying with Ti and Zr. Indeed, within a precision of ± 0.5 eV, no shift is observed for Ti and Zr with respect to the pure elements. In contrast, a shift of about 0.8 eV is established for Ni.

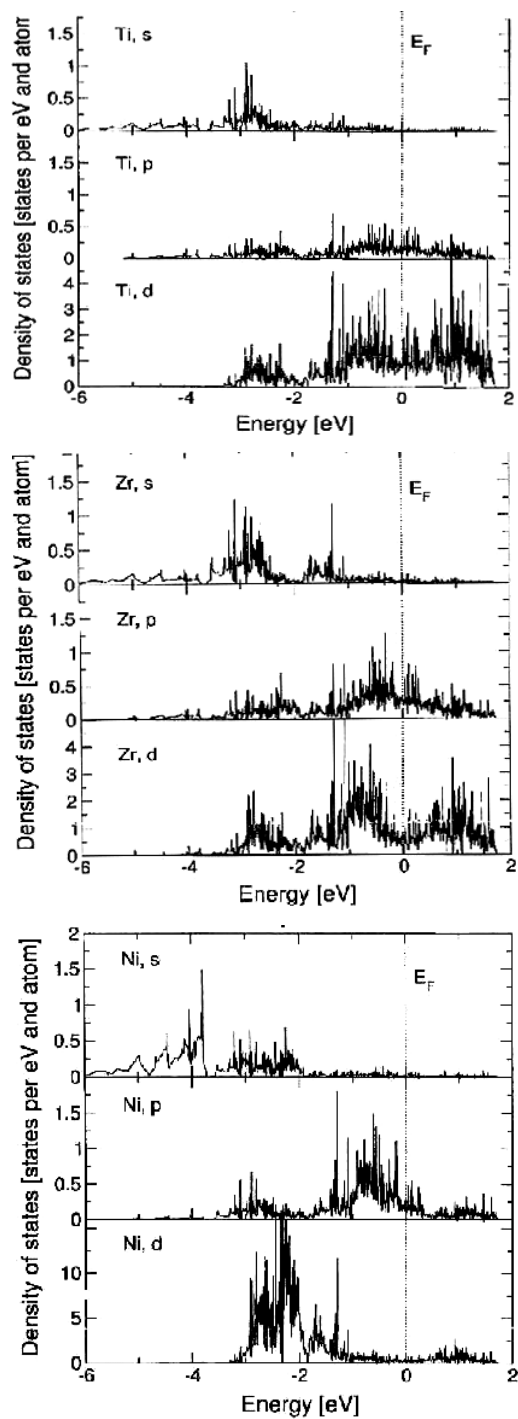


Figure 12. Partial DOSs for Ti (upper panel), Zr (middle panel), and Ni (lower panel), in $W-Ti_{52}Zr_{32}Ni_{16}$. The origin is set at the Fermi level.

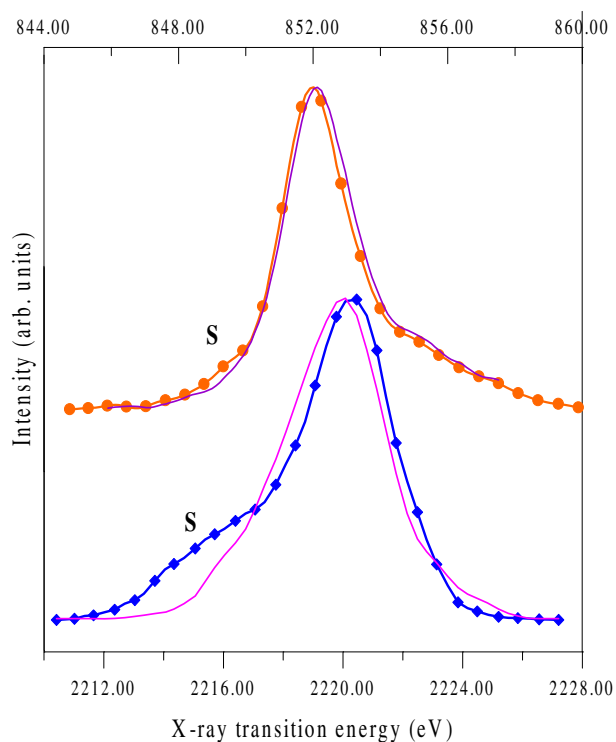


Figure 13. Occupied Zr (lower curves and lower energy axis) and Ni (upper curves and upper energy axis) d states in *i*-Ti-Zr-Ni (full curves) and *i*-Ti-Zr-Ni:H (symbols).

The calculation also shows that E_F lies in a valley of the DOS at about 0.1 eV from the minimum. Note that a DOS calculation using the TB-LMTO method performed for a 1/1 approximant of composition $\text{Ti}_{46}\text{Zr}_{37}\text{Ni}_{17}$ concluded that there is a clear pseudogap whose minimum is slightly shifted from E_F (Fournée *et al* 2000a). In fact, high-resolution PES measurements using a UV source and a sample of nominal composition $\text{Ti}_{46}\text{Zr}_{37}\text{Ni}_{17}\text{Pd}$ indicated a strong depletion of the total DOS at E_F (Fournée *et al* 2000b).

XAS measurements on the unoccupied p and s-d states of Ti, Zr, and Ni in *i*- $\text{Ti}_{53}\text{Zr}_{27}\text{Ni}_{20}$ are fairly consistent with the DOS calculations. The same studies have been carried out on *i*- $\text{Ti}_{45}\text{Zr}_{38}\text{Ni}_{17}$ with 1.4 H. Upon hydrogenation, for all elements, the absorption edges are shifted towards high energies and additional states are observed that have been ascribed to mixing with H s states. An indication has also been given by a Zr s-d empty-states investigation that the localized character of the empty d states goes on increasing upon hydrogenation (Belin-Ferré *et al* 2001).

To date, Zr and Ni occupied d states in *i*-TiZrNi and *i*-TiZrNi:H have only been measured comparatively (figure 13), in XES experiments. A feature towards low transition energies, labelled S in figure 13, has been ascribed to additional states due to hybridization between Zr(Ni) d and H s states. The relative intensity of this feature in the Zr spectrum is much higher than in the Ni spectrum, which suggests that H bonds preferentially to Zr although bonding with Ni also exists (Belin-Ferré *et al* 2001).

(d) Al–Mg- or Mg-based systems

QCs and approximant structures have been found to exist also in Franck–Kasper-type systems such as Al–Mg–Zn and Mg–Zn rare-earth (RE) alloys—namely, systems without TM (or d) atoms. The Al–Mg–Zn system is an interesting one, although its electronic properties are not as remarkable as for Al–Cu(Pd)–TM phases since for instance the resistivity at room temperature of the i-compound is rather similar to that of amorphous metals (it ranges around 40–70 $\mu\Omega$ cm). Indeed, there are approximants that may be prepared by partial substitution of Zn for Al (Takeuchi and Mizutani 1995, Mizutani *et al* 1997) or for which DOS calculations are feasible. On the other hand, Mg–Zn–RE may have potentially interesting magnetic properties. Therefore, some attention has been paid to these Al–Mg–Zn and Mg–Zn–RE compounds.

Calculations have been carried out on Al–Mg–Zn approximant structures and related crystalline phases by Hafner and Krajci (1992, 1993) and Sato *et al* (1995) and Mizutani *et al* (2001). Both calculations use the LMTO-ASA method. They revealed that the DOS is dominated by an intense Zn d band located far from E_F , around 10 eV below. This d band is mixed with Mg and Al s and p states that form a rather flat wide band. In the vicinity of E_F , p states mainly arising from Al are present and E_F falls in a dip of the DOS but not exactly at the very minimum (figure 14). Note that Mizutani *et al* (1998) showed that on changing the nominal composition of the approximant, namely for $\text{Al}_x\text{Mg}_{40}\text{Zn}_{60-x}$ and $15 < x < 53$, the pseudogap does not change appreciably, but E_F moves across it. Such results are in agreement with PES measurements by Takeuchi and Mizutani (1995) on the series of $\text{Al}_x\text{Mg}_{40}\text{Zn}_{60-x}$ approximants mentioned above. XES experimentation on the same samples is in progress. However, from first experiments, differences are observed in the shapes and energy extents of the partial spectral curves from quasicrystalline to 1/1- and 2/1-approximants in this system, which indicates modifications in the electronic interactions according to the atomic structure and nominal composition of the specimen.

Calculations of the DOS for a Mg–Zn–Y approximant are available nowadays (Krajci and Hafner 2000, Ishii 2001) and experiments are in progress on this system whose results will be reported elsewhere. Preliminary data from x-ray spectroscopy measurements have shown a continuous decrease of the metallic character from pure Mg to Zn_2Mg , an approximant of hexagonal structure, and i-Zn–Mg–Y. Note that a small pseudogap at E_F is expected from DOS calculations for the approximant, whereas it is not yet clearly established from the experimental investigation based on XES and XAS.

3. Decagonal quasicrystals

QCs exist also in an atomic arrangement which is quasiperiodic in two dimensions and periodic in the third one. Such a QC can be considered as being a periodic stacking along the axis c of layers that are quasiperiodic in the plane perpendicular to c . They are the so-called decagonal QCs; their diffraction patterns clearly exhibit tenfold symmetry. The first decagonal phase, which was metastable, was discovered in the Al–Mn system by Bendersky (1985); since then, d-QCs—either stable or metastable phases—have been recognized in many binary or ternary (quaternary) systems. Approximant phases exist also whose local structure is similar to that in d-QCs and can be seen as a packing of column clusters each exhibiting fivefold symmetry. Details about the atomic structure can be found in Steurer and Haibach (1999), Boudard and de Boissieu (1999), or Boudard (2000). Note that d-QCs display some anisotropy of their electronic properties that is related to the twofold periodic–quasiperiodic atomic arrangement. To give an example, the electric conductivity is metallic along the periodic axis and similar to that of i-compounds in the quasiperiodic layers (Martin *et al* 1991, Edagawa *et al* 1996).

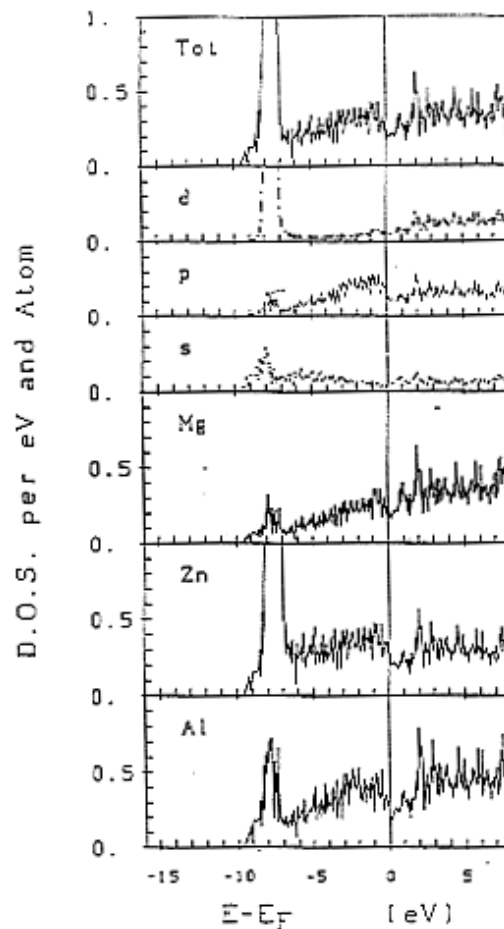


Figure 14. Total and partial DOSs of a model i-Al-Mg-Zn QC. The DOS is clearly dominated by Zn d states with very slight sp-d hybridization at E_F .

The DOS calculations for d-Al-Cu-Co by Trambly de Laissardière and Fujiwara (1994b) as well as Krajci *et al* (1997a) were based principally on the structural models proposed by Burkov (1991, 1992, 1993). Not surprisingly, they have shown that the DOS is dominated by Cu d states that lie in the middle of the occupied band, whereas Co states are closer to E_F (figure 15). Results for d-Al-Ni-Co (Krajci *et al* 2000) are very much dependent on the way in which the chemical decoration of the structural models is achieved, which may even lead to contradictory results. Here, comparison with the experimental data that are reported below has been essential to assess the validity of the structural model. The most important issue regarding these calculations for the model that fits well with experimental SXS data is that the d states of Ni and Co, via hybridization with Al, interact in such a way that they repel each other. As a result, there is no clear pseudogap in the total DOS of this system although it is present in the Al states. DOS calculations are also available for d-Al-Pd-Mn (Krajci *et al* 1997a), founded on tiling the quasiperiodic plane with pentagonal stars, decagons, and compacted hexagons according to the model proposed by Hiraga and Sun (1993). An example of a calculated DOS is displayed in figure 16, for two decorations of a d-Al-Pd-Mn approximant. Finally, for all

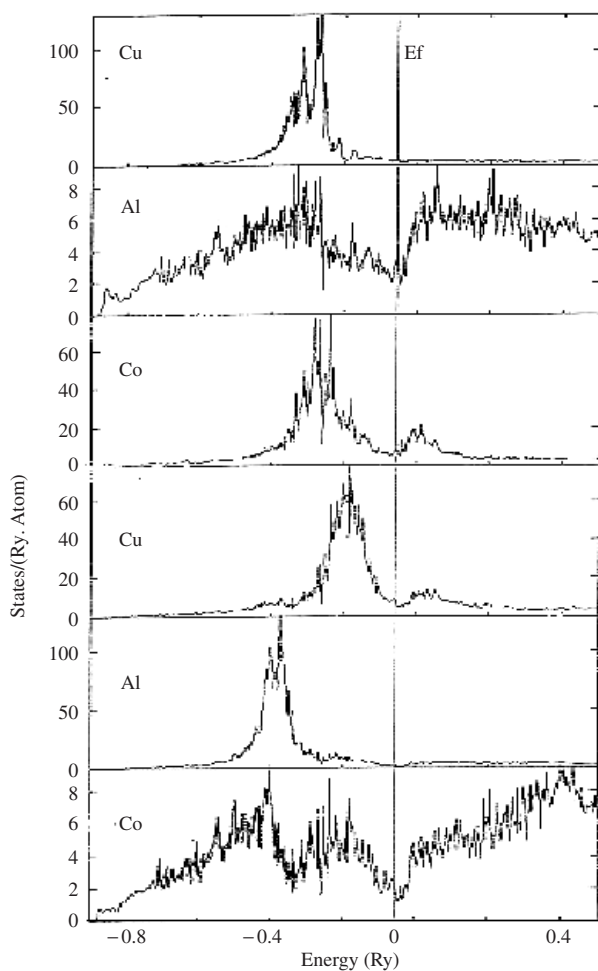


Figure 15. The DOS of a model of d-Al–Cu–Co. From top to bottom, Cu, Al, and Co in large (three upper panels) and small clusters (three lower panels) (Trambly de Laissardière and Fujiwara 1994b).

these systems, the main conclusions of the calculations are:

- (i) a pseudogap always forms at E_F in the Al sub-bands;
- (ii) sp–d hybridization plays a significant role in the formation of this pseudogap.

Experimental data also exist for many d-QCs. For d-Al₆₅Cu₂₀Co₁₅, PES and SXES have corroborated the energy ranges where the Cu and Co d states are present, in agreement with the calculated DOS (Stadnik *et al* 1995, Belin-Ferré *et al* 1996). In addition, XES has ascertained a significant depletion of the Al DOS at and around E_F , thus confirming the formation of a pseudogap in the Al states; it also indicated hybridization of the Al s–d and p states below E_F with Co d states (figure 17).

PES measurements performed at room temperature with 0.3–0.4 eV energy resolution for d-Al₇₀Ni₁₅Co₁₅ show essentially an intense broad peak located about 2 eV below E_F and no pseudogap in the total valence band (Depero and Parmigiani 1993, Stadnik *et al* 1995,

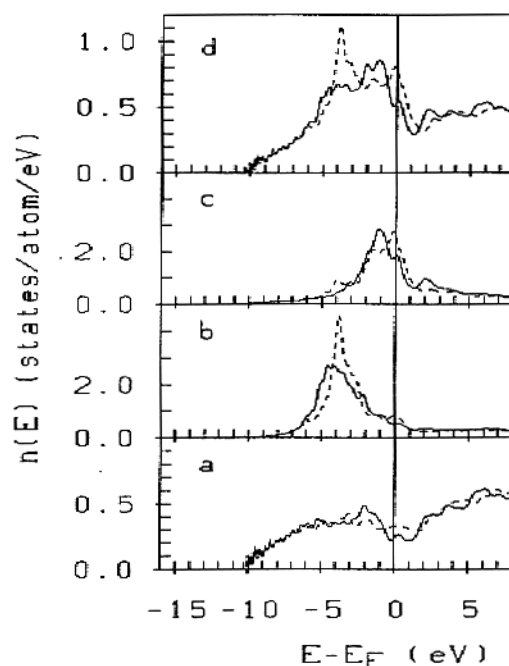


Figure 16. Al (a), Pd (b), Mn (c), and total (d) DOSs for two variants (full and dashed curves) of the structure of an approximant of the d-Al-Pd-Mn QC (Krajci *et al* 1997a).

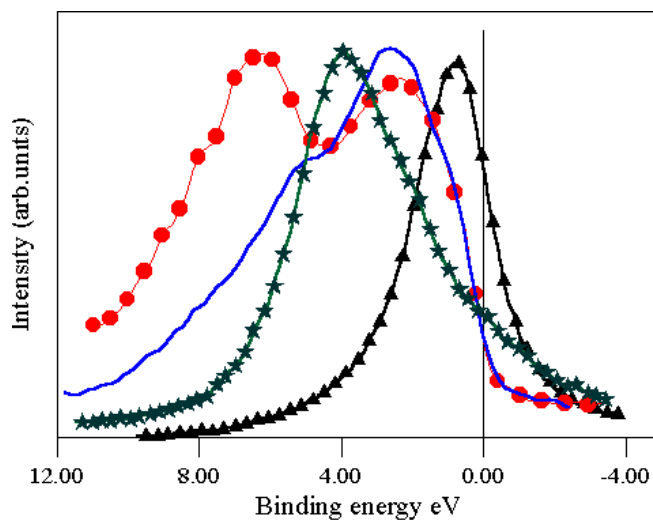


Figure 17. The valence band in d-Al-Cu-Co: the partial electronic distributions are: Al 3s-d: curve with full circles; Al 3p: full curve; Co 3d-4s: starred curve; and Co 3d-4s: curve with triangles.

1997). Conversely, various forms of d-Al-Ni-Co (d-Al₇₂Ni₂₀Co₈, d-Al₇₀Ni₁₇Co₁₃, and d-Al_{72.5}Ni₁₃Co_{14.5}) have been probed using XES (Fournée 1998) (figure 18). In such experi-

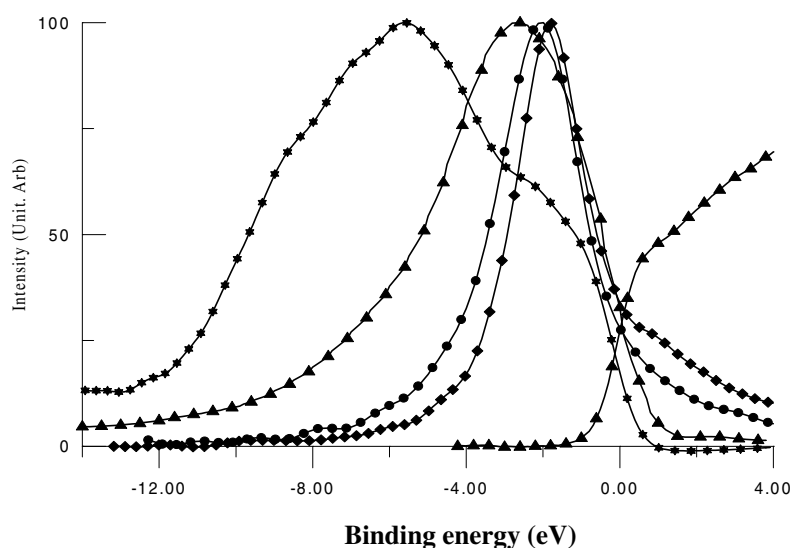


Figure 18. d-Al₇₀Ni₁₇Co₁₃. Left-hand-side curves: Al 3s-d (stars), Al 3p (triangles), Ni 3d-4s (dots), Co 3d-4s (diamonds).

ments, for each element the data average the contributions due to periodic and non-periodic atomic sites. The TM d states are found in an energy range around 2 eV below E_F . In the sample of d-Al₇₂Ni₂₀Co₈, within the experimental precision, the two Co d and Ni d state contributions overlap almost totally. This is no longer true for the two other samples, where the Ni d states are pushed a little towards the centre of the occupied band while the Co d states move closer to E_F (figure 18). Indeed, the maximum of the Ni d distribution is at 2.06 ± 0.1 eV for d-Al₇₂Ni₂₀Co₈ against 1.90 ± 0.1 eV for d-Al₇₀Ni₁₇Co₁₃ and d-Al_{72.5}Ni₁₃Co_{14.5}. This clearly shows that d states in the two TMs repel each other, in agreement with Krajci *et al* (2000) DOS calculations.

4. Quasicrystal surface electronic structure

Insight into the electronic structure of QC surfaces is of great interest, since many properties such as friction, tribology, and wetting (Thiel *et al* 1999, Dubois *et al* 2000) that may have industrial potentialities involve the very surface; in particular, it is important to assess whether the surface electronic structure is similar or not to that of the bulk compounds. The theoretical data reported in the previous sections relate always to bulk materials. As far as experiments are concerned, the XES and XAS results basically apply to the bulk specimen, whereas some contribution due to occupied surface states is involved in PES. From accurate investigation of the valence band edges at low temperature, it is clear that the pseudogap existing in the bulk QC compounds persists close to the surface. But what about the very surface? A theoretical study of the influence of the surface on the character of the electronic states using the tight-binding approximation for a three-dimensional structural model of a QC based on the Penrose tiling led Janssen and Fasolino (1998) to speculate that the pseudogap should exist at the very surface, in agreement with Rivier (1993).

There are various experimental means to gain insight into the surface electronic structure. However, for QCs an additional problem arises from whether the real surface is quasicrystalline

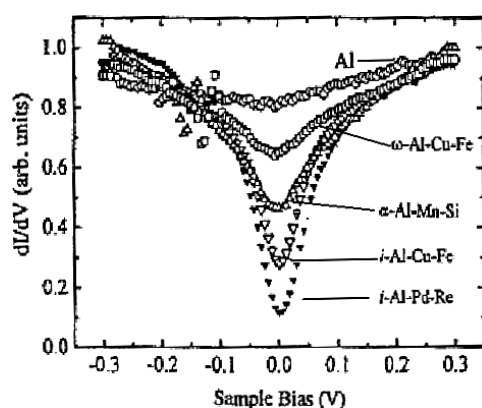


Figure 19. Tunnelling spectra for fcc Al, crystalline ω -Al₇Cu₂Fe, the α -Al-Mn-Si approximant, and two QCs: i-Al-Cu-Fe and i-Al-Pd-Re (Davydov *et al* 1996).

or not; indeed, contradictory results were obtained from PES measurements performed at energies for which the contribution of surface states is significant, according to the way in which the surface was prepared—either cleaved or sputter-annealed (Stadnik *et al* 1996, Neuhold *et al* 1998). Many investigations have been carried out, particularly using single i-AlPdMn and i-AlCuFe grains, in order to study the very surface of specimens to secure a procedure allowing one to achieve real surface quasiperiodicity (see Thiel *et al* (1999) and references therein, Chevrier (2000) and references therein).

Direct evidence of the persistence of a pseudogap in the total DOS at the surface of i-Al-Cu-Fe, i-Al-Pd-Mn, i-Al-Pd-Re was obtained from point contact and tunnelling spectroscopy measurements at low temperature, that involve the very surface of well characterized specimens. Comparison with approximant and conventional metallic alloys or fcc Al has shown that the width of the pseudogap in the QCs is about 50 meV and may be as large as 0.4 eV in i-Al-Pd-Re (figure 19). The pseudogap at the surface has been found to be deeper for the QCs than the approximant, and also deeper for the more resistive QC (Davydov *et al* 1996, Escudero *et al* 1998). Note that previous study of i-Al-Cu-Fe thin films revealed the presence of a pseudogap at about 4 K that was 60 meV in width (Klein *et al* 1995).

A reduced local DOS at E_F was also derived from inspection of the shape of TM 2p core level lines in i-AlPdMn and i-AlCuFe, as compared to pure TM metals, by Fournée *et al* (2000c, 2002). The Mn 2p_{3/2} line for a single grain of icosahedral Al₇₀Pd₂₁Mn₉ is more than 1 eV narrower than for pure Mn metal or β -cubic Al₆₀Pd₂₅Mn₁₅ (Jenks *et al* 1996). Let us note that the remarkable sharpness of the Mn 2p_{3/2} line was taken as a signature of the quasicrystalline order at the surface of icosahedral Al-Pd-Mn. The same is true for the Fe 2p lines of the compounds. Such a narrowing is certainly responsible for the decrease of the full width at half-maximum intensity observed from Mn d and Fe d XES spectra, as reported in section 2. In addition, Fournée *et al* (2002) observed that the Mn and Fe 2p lines do not display the large asymmetric tail that they exhibit for metallic systems. For metals, the asymmetry of the core level line is directly connected to a sharp Fermi edge in the valence band spectra; therefore the loss of the asymmetric tail is attributed to a decrease in the local DOS at E_F . Note that the 2p levels of Cu and Pd were also found to be narrower than for pure metals but not as much as for Mn and Fe states. This is consistent with the conclusions deduced for Mn and Fe 2p, since the Cu and Pd bands lie far from E_F ; therefore their contribution to the total DOS at E_F is significantly low. Also, the authors observed that the Mn 2p linewidth was increased for

an i-Al–Pd–Mn sample prepared by fracture in ultrahigh vacuum, thus verifying the results obtained by Neuhold *et al* (1998) indicating metallic character of such cleaved surfaces.

5. Origin of the pseudogap

We have already mentioned that a HR stabilization mechanism and sp–d hybridization at E_F have been proposed as responsible for the depletion in the DOS around E_F . The HR criterion has been used particularly by Tsai, who discovered most of the stable ternary QCs known so far, especially Al-based ones, and recently the binary stable i-Cd–Yb compound. To investigate the roles of the HR and sp–d hybridization criteria in more detail, Al 3p occupied states were studied more specifically in a series of crystalline Al–Cu alloys as well as conventional compounds and approximants of the Al–Cu–Fe system, all of the HR type with variable structure and size of the Brillouin zone. The methodology was the same as described above for investigating QCs on the basis of XES experiments. Comparison was made with i-Al–Cu–Fe. For each specimen a pseudogap at E_F was observed in the Al sub-bands which, within the experimental accuracy, was found to be the same irrespective of the composition and structural complexity for the Al–Cu samples. This pseudogap was more marked for the HR specimens containing Fe (Belin-Ferré *et al* 1997, 2000, 2001, Fournée *et al* 1998 and Fournée 1998), thus indicating a role of the Al–Fe interaction near E_F in Al–TM intermetallics in agreement with Trambly de Laissardière and Mayou (1997). The pseudogap was also found to be progressively more marked when going from 1/1 cubic to rhombohedral, orthorhombic, and pentagonal approximants, and to the icosahedral compound. Note that the pentagonal approximant is the closest to the QC. The values of the intensity at E_F of the Al 3p distribution within the framework of the normalization procedure described in section 2 are shown in figure 20 versus the electron-to-atom ratio. These results have been calculated using the values determined by Raynor (1959), namely 3 for Al, 1 for Cu, and –2 for Fe. Clearly the lower intensities, i.e. deeper pseudogaps, are found for i-compounds and their closest approximants. In the Al–Li–Cu system, where there is no Al–TM interaction near E_F , there is a significant pseudogap in the Al states (almost as large as for icosahedral Al–Cu–Fe) for both i-compounds and approximant compounds (Belin-Ferré *et al* 1997).

The HR criterion leads to strong stability for the so-called HR compounds due to the importance of the energy term, as demonstrated by Jones (1937, 1962). It is written as

$$\int EN(E) dE. \quad (1)$$

In order to bring the spectroscopy energy data together with thermodynamics and theoretical DOS calculations, a minus sign has been inserted in the right-hand side of equation (1) since energies are quoted as positive on the side of the valence band by convention in XES measurements. The integration is therefore made from the Fermi energy over the whole energy range covered by the valence band, and the moments of order 1 of the contributions of the various partial electronic distributions to the valence band are written as

$$-\sum \int EN(E) dE / \int N(E) dE. \quad (2)$$

The quantity in the denominator is used for normalization purposes. For the Al–Cu–Fe compounds, the contributions to the total energy of the various partial DOSs are calculated according to equation (2) by substituting in the appropriate experimental $N(E)$ data. Hence, the mean binding energy $M1$ of the Al 3p states represents only one of the contributions to the total energy of the compound. However, it is the one that varies significantly within the composition field around the QC concentration, since Fe d states do not change significantly

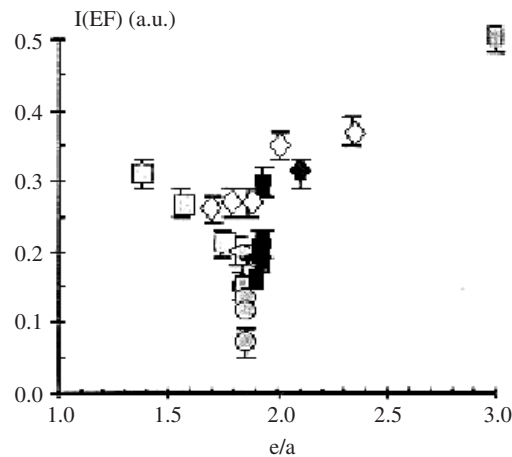


Figure 20. Intensity at the Fermi level versus electron per atom ratio for fcc Al (grey rectangle), HR Al–Cu crystals (diamonds), Φ -Al₁₀Cu₁₀Fe (flattened diamonds), ω -Al₇Cu₂Fe (full diamonds), β -AlCuFe crystals (squares), AlCuFe approximants (narrow dark rectangles), and i-QCs (full circles).

from one specimen to another. Figure 21 shows a plot of $M1$ for the Al 3p DOS as a function of the electron-to-atom (e/a) ratio. It clearly presents a minimum for the i-AlCuFe compound which corresponds to $e/a = 1.86e^-/\text{atom}$. The existence of the minimum of $M1$ for Al 3p (it was verified that it also exists for the Al 3s–d DOS at the position of the icosahedral compound) shows that the major contribution to the stability of the i-AlCuFe QC is due to HR scattering of nearly free Al states (Belin-Ferré *et al* 2000, 2001).

On the other hand, recently, Mizutani *et al* (2002) have calculated within the framework of the LMTO-ASA method the dispersion relations, the Fermi surface, and the local electronic distributions for the nearly free-electron-like Frank–Kasper AlMgZn approximant whose structure was derived from the Rietveld method applied to x-ray diffraction spectra. These authors pointed out that in this alloy where there is no sp–d hybridization effect at E_F , the pseudogap across E_F originates from a HR scattering-type interaction associated with specific planes. The shallow pseudogap obtained is similar to the one in HR AlCu phases derived from XES measurements (Belin-Ferré *et al* 1997, Fournée *et al* 1998)

To quantify the importance of the sp–d hybridization at E_F , the moment of order 2, $M2$, of the Al 3p distribution was also computed for all these samples, taking advantage of the result from tight-binding theory that the second moment $M2$ of the partial DOS at a site i is the sum $\sum t_{ij}^2$ over all neighbours j of the amplitudes t_{ij} for hopping between the sites i and j (Belin-Ferré *et al* 2000). This is written as

$$M2 = \int E^2 N(E) dE / \int N(E) dE \quad (3)$$

Hence, the higher the number Z of first neighbours, the higher $M2$, because the number of hopping channels from site i to its neighbours is increased. One also expects the strong hybridization between two neighbour sites to increase $M2$ due to a larger overlap of the wavefunctions at each site. This effect can be detected when comparing structures with different interatomic distances or higher hybridization of Al with d metal states. Therefore, one expects $M2$ to vary with the coordination number Z around Al sites. This trend is actually

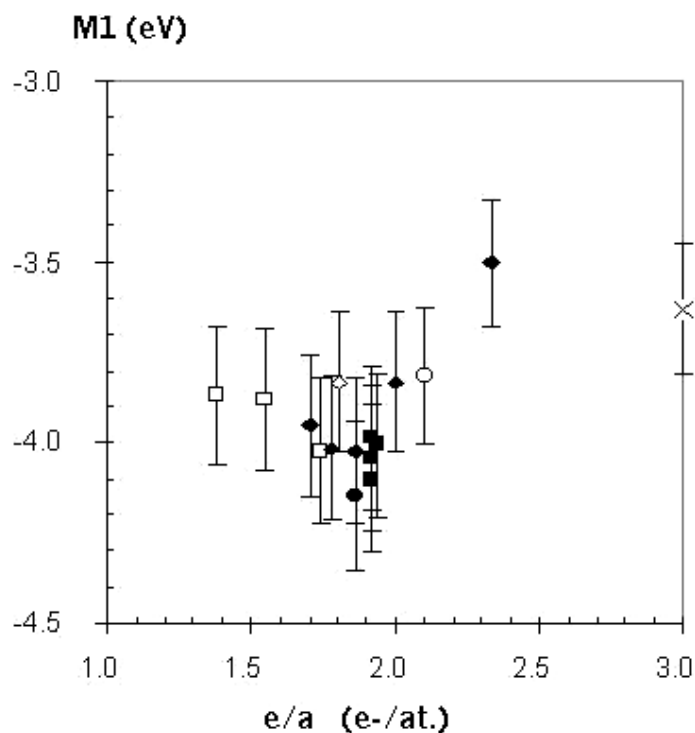


Figure 21. Moment of order 1 of the Al 3p distribution versus electron per atom ratio for the same samples as in figure 20. The symbols are as in figure 20.

shown in figure 22. These data are discussed in more detail in Belin-Ferré *et al* (2000, 2001). The difference observed between conventional alloys (the lower line in figure 22) and the i-QC compounds and close approximants (the upper line—with a higher $M2$ -value than for the conventional crystal with same Z) confirms a stronger hybridization between Al 3p and Fe 3d states in the i-compounds.

All these observations confirm the interplay between the HR scattering mechanism and sp-d hybridization at E_F in Al-Cu(Pd)-TM QCs and closely related approximants, that results in the formation of a larger pseudogap in these compounds. Hence, the stabilization mechanism of QCs and approximants is enhanced with respect to that for related conventional compounds. The results reported in sections 2 (c) and 2 (d) suggest that this conclusion may be extended to the Mg-based QCs and to Ti-Zr-Ni compounds as well. The remaining question that is still without an answer is that of why Nature prefers to stabilize such apparently complicated atomic structures rather than simpler ones—for instance cubic structures.

6. Conclusions

All the results presented in this article have been confirmed by many experimental techniques other than XES, XAS, and valence band studies by means of PES, such as specific heat measurements, resistivity and conductivity measurements, electron energy-loss studies, and AS. To give examples, let us mention: that very weak plasmon energy losses due to the excitation of Al 3p electrons were observed in core level PES spectra of i-Al₇₀Pd₂₀Mn₁₀,

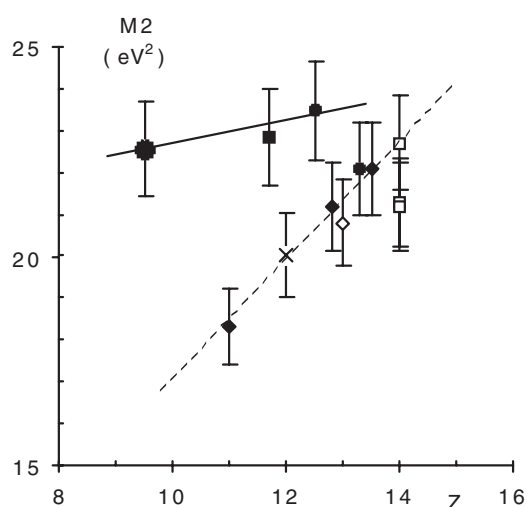


Figure 22. Moment of order 2 of the Al 3p distribution versus the coordination number Z . Dotted line: the cross is for fcc Al, solid diamonds are for Al-Cu HR phases, the open diamond is for Φ -Al₁₀Cu₁₀Fe, the open circle is for ω -Al₇Cu₂Fe, open squares are for β -cubic CsCl-type Al-Cu-Fe phases. Top solid line: the full line corresponds to i-Al-Cu-Fe, the solid square to its orthorhombic and rhombohedral approximants, and the open circle is for an i-Al-Pd-Mn compound.

confirming that Al states have lost the nearly free-electron character that they have in fcc Al (Zurkirch *et al* 1996, 1997); and that optical studies of i-Al₇₀Pd₂₁Mn₉ reported similarities with other materials which actually present a true energy gap (Degiorgi *et al* 1993) and that highly structurally ordered i-Al₇₀Pd₂₀Mn₁₀ resembles Al₂Ru which is reminiscent of semiconductors in the high-frequency range. Thus, altogether, a fair consensus has been obtained by means of theoretical investigations and many experimental techniques. These results for QCs and approximants as compared to conventional crystals of the same phase diagrams may be summarized as follows:

- (i) the occurrence of a pseudogap at E_F that is also present at the very surface has been well established for i-QCs whose formation derives from both HR and Al-TM hybridization effects;
- (ii) the pseudogap does not exist in the total DOSs of decagonal QCs but always exists in the Al sub-bands;
- (iii) states in QCs and close approximants are of more localized-like character in the vicinity of the pseudogap at E_F than in the usual intermetallics and at greater distances, above as well as below E_F , they are extended-like in character, signalling a clear tendency to weak electron localization especially effective on either side of the pseudogap.

Accordingly, there is a progressive loss of the metallic character when going from usual crystals to approximants and QCs, that in turn may allow one to tune the metallic character through a series of compounds as has been done recently in investigating the surface energy of QCs with respect to water (Dubois *et al* 2000 and 2002).

To finish, let us underline that, as already mentioned, the experimental data reported in this article agree rather well with the model of recurrent localization due to a hierarchy of clusters proposed by Janot and de Boissieu (1994) and Janot (1996, 1997) for describing the

structure of i-Al–Pd–Mn. This model proposes that so-called PMI Mackay clusters with the central shell built with eight or nine Al atoms, surrounded by interpenetrating shells of Mn, Pd, and Al atoms, scale hierarchically according to the inflation ratio τ^3 (τ^3 is the golden number), with the result that, in real space, the volumes scale as τ^9 . The first step consists in forming the PMI unit. In the second step, PMI clusters are arranged in such a way as to form a cluster of PMI clusters that keeps the same arrangement as in the elemental PMI, and so on. Within this atomic arrangement, the electrons are energetically confined mostly in the occupied band, with an almost vanishingly flat free-electron-like conduction band.

Acknowledgments

Thanks are due to the many colleagues and friends with whom I worked and had fruitful enlightening discussions with; I would especially like to mention here Zoltan Dankhazi, Vincent Fournée, Jean Marie Dubois, Anne Sadoc, Dimitris Papaconstantopoulos, Guy Trambly de Laissardière, Didier Mayou, Claire Berger, Uichiro Mizutani, Jürgen Hafner, Takeo Fujiwara, Yasushi Ishii, Mehmet Erbudak, Ken Kelton, Patricia Thiel and Cynthia Jenks. Some data reported in this article were obtained with Herbert Müller, thanks to an Austrian East–West Co-operation programme under the title ‘Soft x-ray spectroscopy of metallic systems’.

References

- Agarwal B K 1979 *X-Ray Spectroscopy (Optical Series)* (Berlin: Springer) p S987
 Bahadur D, Gaskell P H and Imeson D 1987 *Phys. Lett. A* **120** 417
 Belin E, Dankhazi Z, Sadoc A and Dubois J M 1994 *J. Phys.: Condens. Matter* **6** 8771
 Belin E, Dankhazi Z, Sadoc A, Flank A M, Poon J S, Müller H and Kirchmayr H 1995 *Proc. 5th Int. Conf. on Quasicrystals* ed C Janot and R Mosseri (Singapore: World Scientific) p 435
 Belin E, Kojnok J, Sadoc A, Traverse A, Harmelin M, Berger C and Dubois J M 1992 *J. Phys.: Condens. Matter* **4** 1057
 Belin E and Mayou D 1993 *Phys. Scr. T* **49** 356
 Belin E and Traverse A 1991 *J. Phys.: Condens. Matter* **3** 2157
 Belin-Ferré E 1999 *Quasicrystals (Mater. Res. Soc. Symp. Proc. vol 553)* ed J M Dubois, P A Thiel, A P Tsai and K Urban (Warrendale, PA: Materials Research Society) p 347
 Belin-Ferré E, Dankhazi Z, Sadoc A, Berger C, Müller H and Kirchmayr H 1996 *J. Phys.: Condens. Matter* **8** 3513
 Belin-Ferré E and Dubois J M 1996 *J. Phys.: Condens. Matter* **8** L717
 Belin-Ferré E, Fournée V and Dubois J M 1997 *New Horizons in Quasicrystals Science: Research and Applications* ed A Goldman, P A Thiel, D Sordelet and J M Dubois (Singapore: World Scientific) p 9
 Belin-Ferré E, Fournée V and Dubois J M 2000 *J. Phys.: Condens. Matter* **12** 8189
 Belin-Ferré E, Fournée V and Dubois J M 2001 *Mater. Trans.* **42** 911
 Belin-Ferré E, Hennig R, Dankhazi Z, Sadoc A, Kim Y and Kelton K F 2002 *Proc. Quasicrystals 2001* at press
 Berger C 1994 *Lectures on Quasicrystals* ed F Hippert and D Gratias (Les Ulis: Les Editions de Physique) p 463
 Berger C, Belin E and Mayou D 1993 *Ann. Chim. Fr.* **18** 485
 Bendersky L 1985 *Phys. Rev. Lett.* **55** 1461
 Bonnelle C 1987 *Ann. Rep. R. Soc. Chem. Lond.* p 201
 Boudard M 2000 *Quasicrystals; Current Topics* ed E Belin-Ferré, C Berger, M Quiquandon and A Sadoc (Singapore: World Scientific) p 73
 Boudard M and de Boissieu M 1999 *Physical Properties of Quasicrystals* ed Z Stadnik (Berlin: Springer) p 91
 Bruhwiller P A, Wagner J L, Biggs B D, Shen Y, Wong K M, Schnatterly S E and Poon S J 1988 *Phys. Rev. B* **37** 6529
 Burkov S E 1991 *Phys. Rev. Lett.* **67** 614
 Burkov S E 1992 *J. Physique* **2** 695
 Burkov S E 1993 *Phys. Rev. B* **47** 12 325
 Chattopadhyay K, Ranganathan S, Subbana G N and Thangaraj N 1985 *Scr. Metall.* **19** 767
 Chevrier J 2000 *Quasicrystals; Current Topics* ed E Belin-Ferré, C Berger, M Quiquandon and A Sadoc (Singapore: World Scientific) p 303

- Dankhazi Z, Trambly de Laissardière G, Nguyen Manh D, Belin E and Mayou D 1993 *J. Phys.: Condens. Matter* **5** 3339
- Davydov D N, Mayou D, Berger C, Gignoux C, Neumann A, Jansen A G M and Wygner P 1996 *Phys. Rev. Lett.* **77** 3173
- Degiorgi L, Chernikov M A, Beeli C and Ott H R 1993 *Solid State Commun.* **87** 721
- Delahaye J and Berger C 2002 *Phys. Rev. B* **64** 094203
- Depero L E and Parmigiani F 1993 *Chem. Phys. Lett.* **214** 208
- Dubois J M 2001 *Quasicrystals—Preparation, Properties and Applications (Mater. Res. Soc. Symp. Proc. vol 643)* ed E Belin-Ferré, P A Thiel, A P Tsai and K Urban (Warrendale, PA: Materials Research Society) p K15.1
- Dubois J M, Brunet P and Belin-Ferré C 2000 *Quasicrystals; Current Topics* ed E Belin-Ferré, C Berger, M Quiquandon and A Sadoc (Singapore: World Scientific) p 498
- Dubois J M, Demange V, Bonhomme G, Fournée V, Sordelet D J, Thiel P A and Belin-Ferré E 2002 *Phys. Rev. Lett.* submitted
- Dubost B, Lang J M, Tanaka M, Sainfort P and Audier M 1986 *Nature* **324** 48
- Edagawa K, Yamaguchi S, Suzuki K and Takeuchi S 1996 *Advances in Physical Metallurgy* ed S Banerjee and R V Ramanujan (Amsterdam: Gordon and Breach) p 96
- Ederer D L, Schaefer R, Tsang K L, Zhang C H, Calcott T A and Arakawa E T 1988 *Phys. Rev. B* **37** 8594
- Escudero R, Lasjaunias J C, Calvayrac Y and Boudard M 1998 *J. Phys.: Condens. Matter* **10** 1
- Fournée V 1998 *PhD Thesis* Paris University, unpublished
- Fournée V, Anderegg J W, Ross A R, Lograsso T A and Thiel P A 2002 *J. Phys.: Condens. Matter* **14** 2691
- Fournée V, Belin-Ferré E, Trambly de Laissardière G, Sadoc A, Volkov P and Poon J S 1997 *J. Phys.: Condens. Matter* **9** 7999
- Fournée V, Belin-Ferré E and Dubois J M 1998 *J. Phys.: Condens. Matter* **10** 4231
- Fournée V, Mazin I, Papaconstantopoulos D A and Belin-Ferré E 1999 *Phil. Mag.* **B 79** 205
- Fournée V, Mizutani U and Sato H 2000a private communication
- Fournée V, Mizutani U and Takeuchi T 2000b private communication
- Fournée V, Pinhero P J, Anderegg J W, Lograsso T A, Ross A R, Canfield P, Fisher I R and Thiel P A 2000c *Phys. Rev. B* **62** 14049
- Friedel J 1992 *Helvetica Acta* **61** 638
- Friedel J and Denoyer F 1987 *C. R. Acad. Sci., Paris* **305** 171
- Fujiwara T 1989 *Phys. Rev. B* **40** 942
- Fujiwara T, Kohmoto M and Tokihiro T 1989 *Phys. Rev. B* **40** 7413
- Fujiwara T, Yamamoto S and Trambly de Laissardière G 1993 *Phys. Rev. Lett.* **71** 4166
- Fujiwara T and Yokokawa Y 1991 *Phys. Rev. Lett.* **66** 333
- Hafner J and Krajci M 1992 *Phys. Rev. Lett.* **68** 2321
- Hafner J and Krajci M 1993 *Phys. Rev. B* **47** 11 795
- Hausleitner C and Hafner J 1992 *Phys. Rev. B* **45** 115
- Hiraga K and Sun W 1993 *Phil. Mag. Lett.* **67** 117
- Hüfner S 1995 *Photoelectron Spectroscopy* 2nd edn (Berlin: Springer)
- Ishii Y 2001 private communication
- Ishimasa T, Nissen H-U and Fukano Y 1985 *Phys. Rev. Lett.* **55** 511
- Janot C 1996 *Phys. Rev. B* **53** 181
- Janot C 1997 *J. Phys.: Condens. Matter* **9** 1493
- Janot C and de Boissieu M 1994 *Phys. Rev. Lett.* **72** 1674
- Janssen T and Fasolino A 1998 *Proc. 6th Int. Conf. on Quasicrystals* ed S Takeuchi and T Fujiwara (Singapore: World Scientific) p 756
- Jenks C J, Chang S-L, Anderegg J W, Thiel P A and Lynch D W 1996 *Phys. Rev. B* **54** 6301
- Jones H 1937 *Proc. Phys. Soc.* **49** 250
- Jones H 1962 *J. Physique Radium* **23** 637
- Klein T, Symko O G, Davydov D N and Jansen A G M 1995 *Phys. Rev. Lett.* **74** 3656
- Krajci M and Hafner J 2000 *J. Phys.: Condens. Matter* **12** 5831
- Krajci M, Hafner J and Mihalkovic M 1997a *Phys. Rev. B* **55** 843
- Krajci M, Hafner J and Mihalkovic M 1997b *Phys. Rev. B* **56** 3072
- Krajci M, Hafner J and Mihalkovic M 2000 *Phys. Rev. B* **62** 243
- Krajci M, Windisch M, Hafner J, Kresse G and Mihalkovic M 1995 *Phys. Rev. B* **51** 17 355
- Krause M O and Oliver J H 1979 *J. Phys. Chem. Rev. Data* **8-2** 329
- Kunz C 1979 *Photoemission in Solids* vol 2, ed L Ley and M Cardona (Berlin: Springer) p 299
- Léonard P 1978 *J. Phys. F: Met. Phys.* **8** 467

- Libbert J L, Kelton K F, Gibbons P C and Goldman A I 1993 *J. Non-Cryst. Solids* **153–154** 53
- Macia E and Dominguez-Adame F 2000 *Electrons, Phonons and Excitons in Low Dimensional Aperiodic Systems* (Madrid: Editorial Complutense)
- Martin S, Hebard A F, Kortan A R and Thiel F A 1991 *Phys. Rev. Lett.* **67** 719
- Mayou D 2000a *Quasicrystals; Current Topics* ed E Belin-Ferré, C Berger, M Quiquandon and A Sadoc (Singapore: World Scientific) p 412
- Mayou D 2000b *Phys. Rev. Lett.* **85** 1290
- Mori M, Matsuo S, Ishimasa T, Matsuura T, Kamiya K, Inokuchi H and Matsukawa T 1991 *J. Phys.: Condens. Matter* **3** L767
- Mizutani U, Iwakami W and Fujiwara T 1998 *Proc. 6th Int. Conf. on Quasicrystals* ed S Takeuchi and T Fujiwara (Singapore: World Scientific) p 579
- Mizutani U, Iwakami W, Takeuchi T, Sakata M and Takata M 1997 *Phil. Mag.* **76** 349
- Mizutani U, Takeuchi T, Banno E, Fournée V, Takata M and Sato H 2001 *Quasicrystals—Preparation, Properties and Applications (Mater. Res. Soc. Symp. Proc. vol 643)* ed E Belin-Ferré, P A Thiel, A P Tsai and K Urban (Warrendale, PA: Materials Research Society) p K13.1
- Mizutani U, Takeuchi T and Sato H 2002 *Prog. Mater. Sci.* submitted
- Neuhold G, Barman S R, Horn K, Theis W, Ebert P and Urban K 1998 *Phys. Rev. B* **58** 734
- Nguyen Manh D, Trambly de Laissardière G, Julien J P, Mayou D and Cyrot-Lackmann F 1992 *Solid State Commun.* **82** 329
- Nozières P and de Dominicis C T 1969 *Phys. Rev.* **178** 6105
- Papaconstantopoulos D A 1986 *Handbook of the Band Structure of Elemental Solids* (New York: Plenum)
- Perrot A and Dubois J M 1993 *Ann. Chim. Fr.* **18** 501
- Préjean J J, Berger C, Sulpice A and Calvayrac Y 2002 *Phys. Rev. B* **65** 140203
- Quiquandon M, Calvayrac Y, Quivy A, Faudot F and Gratiás D 1999 *Quasicrystals (Mater. Res. Soc. Symp. Proc. vol 553)* ed J M Dubois, P A Thiel, A P Tsai and K Urban (Warrendale, PA: Materials Research Society) p 95
- Raynor G V 1959 *Prog. Met. Phys.* **1** 19
- Rivier N 1993 *J. Non-Cryst. Solids* **153–154** 458
- Roche S and Fujiwara T 1998a *Aperiodic '97* ed M de Boissieu, J-L Verger-Gaugry and R Currat (Singapore: World Scientific) p 715
- Roche S and Fujiwara T 1998b *Phys. Rev. B* **58** 11 338
- Rooke G A 1968 *J. Phys. C: Solid State Phys.* **1** 767
- Rooke G A 1968 *J. Phys. C: Solid State Phys.* **1** 776
- Rooke G A 1974 *X-ray Spectroscopy* ed L V Azaroff (New York: McGraw-Hill)
- Sadoc A, Belin E, Dankhazi Z and Flank A M 1993 *J. Non-Cryst. Solids* **153&154** 338
- Sato H, Takeuchi T and Mizutani U 1995 *Phys. Rev. B* **64** 94 207
- Schaub T, Delahaye J, Gignoux C, Berger C and Janssen A G M 1999 *J. Non-Cryst. Solids* **250–252** 874
- Schechtman D and Blech I 1985 *Metall. Trans. A* **16** 1005
- Schechtman D, Blech I, Gratiás D and Cahn J W 1984 *Phys. Rev. Lett.* **53** 951
- Sire C 1994 *Lectures on Quasicrystals* ed F Hippert and D Gratiás (Les Ulis: Les Editions de Physique) p 505
- Stadnik Z M, Purdie D, Garnier M, Baer Y, Tsai A P, Inoue A, Edagawa K and Takeuchi S 1996 *Phys. Rev. Lett.* **77** 1777
- Stadnik Z M, Purdie D, Garnier M, Baer Y, Tsai A P, Inoue A, Edagawa K, Takeuchi S and Buschow K H J 1997 *Phys. Rev. B* **55** 10938
- Stadnik Z M, Zhang G W, Tsai A P and Inoue A 1995 *Phys. Rev. B* **51** 11 358
- Steurer W and Haibach T 1999 *Physical Properties of Quasicrystals* ed Z Stadnik (Berlin: Springer) p 51
- Takeuchi T and Mizutani U 1995 *Phys. Rev. B* **52** 9300
- Terakura K 1977 *J. Phys. F: Met. Phys.* **7** 1773
- Terauchi M, Tanaka M, Tsai A P, Inoue A and Masumoto T 1996b *Phil. Mag. Lett.* **74** 107
- Terauchi M, Ueda H, Tanaka M, Tsai A P, Inoue A and Masumoto T 1996a *Proc. 6th Int. Conf. on Quasicrystals* ed S Takeuchi and T Fujiwara (Singapore: World Scientific) p 587
- Thiel P, Goldman A I and Jenks C J 1999 *Physical Properties of Quasicrystals* ed Z Stadnik (Berlin: Springer) p 327
- Trambly de Laissardière G and Fujiwara T 1994a *Phys. Rev. B* **50** 5999
- Trambly de Laissardière G and Fujiwara T 1994b *Phys. Rev. B* **50** 9843
- Trambly de Laissardière G, Dankhazi Z, Belin E, Sadoc A, Nguyen Manh D, Mayou D, Keegan M K and Papaconstantopoulos D A 1995b *Phys. Rev. B* **51** 14035
- Trambly de Laissardière G and Mayou D 1997 *Phys. Rev. B* **55** 2890
- Trambly de Laissardière G, Nguyen Manh D, Magaud L, Julien J P, Cyrot-Lackmann F and Mayou D 1995a *Phys. Rev. B* **52** 7920

- Traverse A, Dumoulin L, Belin E and Sénémaud C 1988 *Quasicrystalline Materials* ed C Janot and J M Dubois (Singapore: World Scientific) p 399
- Tsai A P 1997 *New Horizons in Quasicrystals Science: Research and Applications* ed A Goldman, P A Thiel, D Sordelet and J M Dubois (Singapore: World Scientific)
- Tsai A P, Inoue A and Masumoto T 1987 *Japan. J. Appl. Phys.* **26** 1505
- Tsai A P, Inoue A and Masumoto T 1987 *Japan. J. Appl. Phys.* **26** 1994
- Tsai A P, Inoue A and Masumoto T 1988 *Japan. J. Appl. Phys.* **27** L1587
- Tsai A P, Inoue A and Masumoto T 1989 *Mater. Trans. JIM* **30** 463
- Wang N, Chen H and Kuo K H 1987 *Phys. Rev. Lett.* **59** 1010
- Wang K and Garoche P 1993 *Ann. Chim. Fr.* **18** 475
- Wang K, Garoche P and Calvayrac Y 1988 *Quasicrystalline Materials* ed C Janot and J M Dubois (Singapore: World Scientific) p 372
- Windisch M, Krajci M and Hafner J 1994 *J. Phys.: Condens. Matter* **6** 6977
- Zijlstra E S and Janssen T 2000 *Europhys. Lett.* **52** 578
- Zurkirch M, Atrei A, Hochstrasser M, Erbudak M and Kortan A R 1996 *J. Electron Spectrosc. Relat. Phenom.* **77** 233
- Zurkirch M, DeCrescenzi M, Erbudak M and Kortan A R 1997 *Phys. Rev. B* **56** 10651